Kufa Journal of Engineering
Vol. 17, No. 1, January 2026, P.P. 351-361
Article history: Received 14 March 2025, last revised 22 April 2025, accepted 1 May 2025

EFFECT OF ZRO_2 PARTICLES ON THE MECHANICAL PROPERTIES OF ZR2.5NB ALLOY USED FOR BIOMEDICAL APPLICATION

Ekram Abd Al-Razaq Hassani[1], Ali Hubi Haleem[2], and Haydar H.J. Jamal Al Deen[2]

[1]College of Material Engineering/ Metallurgical Engineering Department, University of Babylon, Iraq, Email:ekramhassani93@gmail.com.

[2] College of Material Engineering/ Metallurgical Engineering Department, University of Babylon, Iraq.

https://doi.org/10.30572/2018/KJE/170119

ABSTRACT

Improving the mechanical properties of biomedical alloys is essential for enhancing their performance and longevity in medical applications. This study investigates the effect of zirconia (ZrO_2) addition on the mechanical behavior of Zr2.5Nb alloy prepared via powder metallurgy. Characterization by scanning electron microscopy (SEM) and mechanical testing (hardness and wear resistance) were employed to evaluate the samples' microstructure, phase composition, and mechanical performance—the addition of 3 wt.% ZrO_2 led to a notable improvement in hardness, increasing from 153 HV (for Zr2.5Nb) to 185 HV (for Zr2.5Nb–3ZrO_2). Furthermore, wear resistance was enhanced, as indicated by a reduced wear rate from 2.39×10^{-7} g/cm³ for the base alloy to 1.88×10^{-7} g/cm³ for the ZrO_2-reinforced alloy under a constant load of 20 N and duration of 40 minutes.

KEYWORDS

Zr-2. 5%Nb alloy; biomedical; mechanical properties; biocompatibility, hardness.

1. INTRODUCTION

Biocompatible is the requirement to select a metallic implant that does not show any toxicity to the surrounding biological system (Gittens et al, 2014). Bones come in a variety of sizes and shapes, including irregular, short, flat, and long, and the shapes and sizes (Narayanan and Seshadri, 2000). The skeletal structure of an adult person is made up of around 206 bony components (Narayanan and Seshadri, 2000). Bones have been arranged isotropically and hierarchically at multiple levels due to their diverse tasks, ranging from loading support to mineral control, including phosphorus and calcium (Kumar, 2017). Zirconium is often utilized in biological applications. The femur knee surface and the head of the hip joints are made of a Zr-2.5 alloy named Oxinium that was advanced by Nephew & Smith in 1997 for TKR and in 2002 for THR (Niinomi, 2015, Di Girolamo, 2014). Despite the resistance of wear of Zirconium is little (due to its low hardness), the oxides of Zr formed in a thin layer when the Zr2.5-Nb alloy is heat-treated at about 500°C in the air (Hou, 2017). The damage to the surface and the removal of materials from the surfaces that are in contact and movement with each other is known as wear. Material may be broken loose as a wear particle, transferred from one surface to another, or damaged at the surface (Antunes and de Oliveira, 2012). The implant's wear properties are substantial, particularly for different joint replacements. Friction between two materials is necessary to understand and discuss the wear. When two solid materials come into contact, contact occurs only at the tips of microscopic protrusions on the surface of each material, meaning that the actual contact area is less than the apparent surface area. For ductile materials, the actual contact area increases when a load is applied. Ductile materials can be welded by compression as a result of plastic joint formation (Kunčická, 2017). These plastic joints are the basic origin of adhesive friction, which occurs when two materials slide over each other. The resistance to shear failure of plastic joints increases the friction force (Antunes and de Oliveira, 2012, Manivasagam, 2010). The wear rate is increasing in case of similar metals are used in contact surfaces. Hence, dissimilar metals will decrease the wear. Specifically, the lower the mutual solid solubility of the metals, the lower the wear. Typical wear coefficients for various conditions (Hyson Jr, 2006).

This research highlights to enhancement of the mechanical properties of Zr2.5Nb alloy by the addition of various percentages of ZrO2(0.5, 1, 1.5, 2, 2.5, and 3)wt. % .

2. MATERIALS AND METHOD

Table 1 and 2, show the metallic powders that used for preparing the alloys with average particle size (measured by using Better size 2000 laser particles size analyzer), purity by XRF analyzer and chemical composition of the alloys. The weighted powders were wetly mixed by using

planetary automatic ball mill, steel balls with various diameters were utilized and the mixing media was Ethanol. The mixing process takes 4 hours.

Table 1. Purity and average particle size of materials

Materials	Purity(%)	Average Particle Size(μm)	Chemical Composition (wt.%)
Zirconium	98.19	14.238	Balance
Niobium	99.79	11.83	2.5
Zirconia	99.8	3.980	(0.5,1,1.5,2,2.5,3)

Table 2. Alloy code and chemical composition

Alloy Code	Chemical Composition
Base	2.5Nb+Balance Zr
B1	0.5ZrO2+2.5Nb+Balance Zr
B2	1ZrO2+2.5Nb+Balance Zr
B3	1.5ZrO2+2.5Nb+Balance Zr
B4	2ZrO2+2.5Nb+Balance Zr
B5	2.5ZrO2+2.5Nb+Balance Zr
B6	3ZrO2+2.5Nb+Balance Zr

3. POWDER COMPACTING

By using an electrical uniaxial hydraulic press type (Soil Test, Inc. USA), the compacting of mixed powders was done. The compaction process includes the following steps:

1- Preparing a die for the compacting process with specific dimensions. The die used in this study is made of stainless steel.

2- Lubricate the die using graphite for the purpose of preventing friction between the die wall and the sample, ease of removing the sample from the die, and avoid cracks that affect the die.

3- Weighing an appropriate amount (5g) of the mixed powder and put it in the die.

4- We use the compaction device for the purpose of obtaining a green sample with dimensions D: 13mm, t: 5mm. Different compaction pressures (600, 650, 700, 750,800 and 850 MPa) with a 4minuts as a period time was used to determine the optimum pressure giving the highest green density.

4. SINTERING

By using a vacuum tube furnace, the sintering process of compacted samples has been done. The sintering process involves the following steps:

1- Heating from room temperature to 500℃.

2- Staying at 500℃ for (2) hours.

3- Heating from 500℃to 1100℃.

4- Staying at 1100℃ for (8) hours.

5- Slow cooling in the furnace with continuous argon conditions to room temperature.

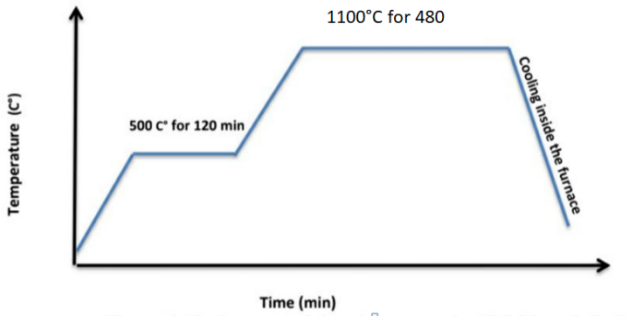

Fig. 1. Program for Sintering Process

5. SAMPLES PREPARATION

The sintering process is followed by grinding of the samples using (180, 400, 600, 800, 1000, 1500, 2000, and 3000). Grit silicon carbide papers are then polished with a diamond to get a bright mirror finish for the final step. The etching solution was Sodium Hydroxide (NaOH). After the etching process, the samples were washed with water and dried.

6. TRUE DENSITY AND POROSITY

According to ASTM B-328 (Tianshuo, 2024), the true porosity of sintered samples was calculated:

1- The specimen is dried up to 100◦C for (5) hours under vacuum conditions, then cooled to room temperature. A refers to the specimen's dry weight.

2- By using an appropriate evacuating pump, which was manufactured for this aim. Over the immersed specimen in oil, the pressure was reduced for (30) minutes at room temperature.

3- Weight the completely impregnated specimens in air, and the weight was B.

4- Weighting the completely impregnated specimens in water (weight F).

5- Lastly, the porosity was gauged by the following equation (Tianshuo, 2024):

$$PF = \left(\frac{B-A}{(B-F)D^{\circ}} * 100\right) Dw \quad (1)$$

$$\rho F = \left(\frac{A}{B-F}\right) * Dw \quad (2)$$

Where:

Dw = density of water (0.995 g/ cm³)

D° = density of oil (0.8 g/ cm³)

7. MICROSTRUCTURE EXAMINATION

7.1. SCANNING ELECTRON MICROSCOPE (SEM)

The microstructure of samples after sintering has been examined by using the scanning electron microscope.

8. HARDNESS MEASUREMENT

The test was carried out using a Brinell hardness tester (Wilson Hard Reichrter UH250). The test consisted of the use of a ball (2.5 mm) diameter and the load used (32.25kg) for 10 seconds

according to ASTM (E10- 15a). Three readings were measured for each specimen, and the average was taken.

9. DRY WEAR TEST

By using a vacuum drying furnace, the specimens were dried at (50 °C) for (2 hours) and cooled in the furnace, and to keep them completely dry, the specimens were saved in well-knit boxes using silica gel. This is done before the wear test.

The dry wear test is investigated by utilizing the pin-on-disk concept using constant radius (4mm) and (400 rpm.) with different sliding distances and (10,15 and 20) N loads. Before the test, by using (0.0001) precision electric balance, the specimen is weighted. After a time of (5, 10, 15, 20, 25, 30, 35, and 40) minutes, the specimen is weighted, and the rate of wear is determined related to equation (4). The test was done according to ASTM G 99 (Sara, 2015). The following equation was used to determine the wear rate (Sara,2015):

$$\text{Wear rate} = \Delta W / \pi r n t \ (\ g/\ N.m.t\ ) \quad (3)$$

Where:

ΔW = Weight lost (g)

t: sliding time(min)

r: the radius of the specimen to the center of the disc (4mm)

n: disc rotation speed(400 rpm)

10. RESULTS AND DISCUTION

10.1. Compacting Pressure

The average particle size of zirconium, niobium and zirconia is shown in Table3.

Table 3. Average Particle Size of elements Powder

Element Powder	Average Particle Size
Zr	14.238
Nb	11.83
ZrO_2	3.980

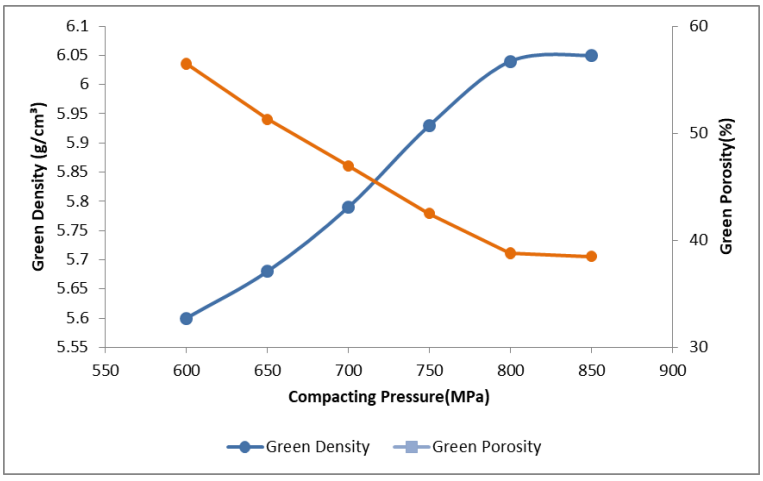

Fig. 2. Influence of Compacting Pressure on Green Density and Green Porosity

10.2. GREEN DENSITY AND GREEN POROSITY

Fig.3. Illustrates effects of adding ZrO_2 on the green density of the alloy. An increase in the proportion of ZrO_2 leads to a reduction in green density. This is because ZrO_2 density is 5.89 g/cm3 and is less than the density of Zr is 6.49 g/cm3; also, the ZrO_2 amount affects on compressibility behavior of the alloy.

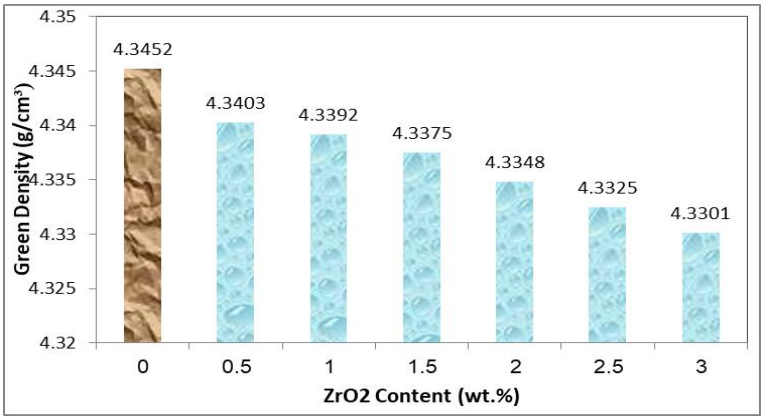

Fig. 3. Effect of ZrO_2 On Green Density

Fig.4 shows the effect of ZrO_2 on green porosity, it can be noted that the porosity decreasing with increasing ZrO_2 content, because the grain size of zirconia smaller than the grain size of zirconium Table 4.

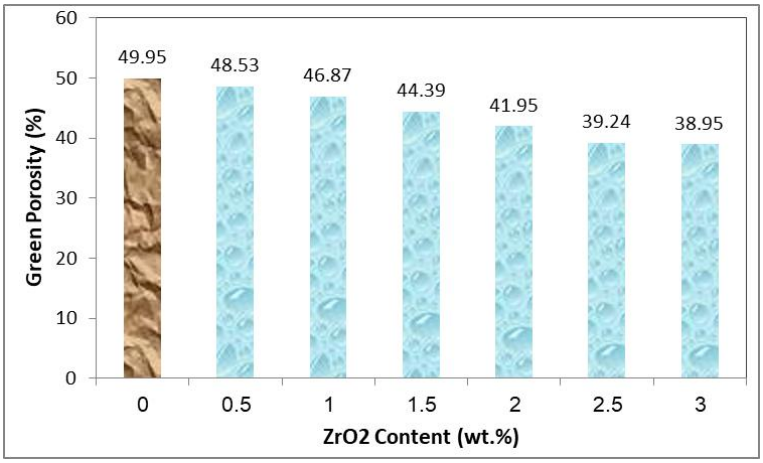

Fig. 4. Effect of ZrO_2 on Green Porosity

10.3. FINAL DENSITY AND FINAL POROSITY

Fig.5 and Fig.6 show the density and porosity after sintering, where the addition of ZrO_2 leads to increasing the density and a reduction in the porosity. The hardness of ZrO_2 is usually higher when compared to the base alloy, so, addition of ZrO_2 particles will affect the densification ability of the alloy containing ZrO_2. The sintering ability of the alloys decreases when the proportion of zirconia is increased, due to the poor diffusion.

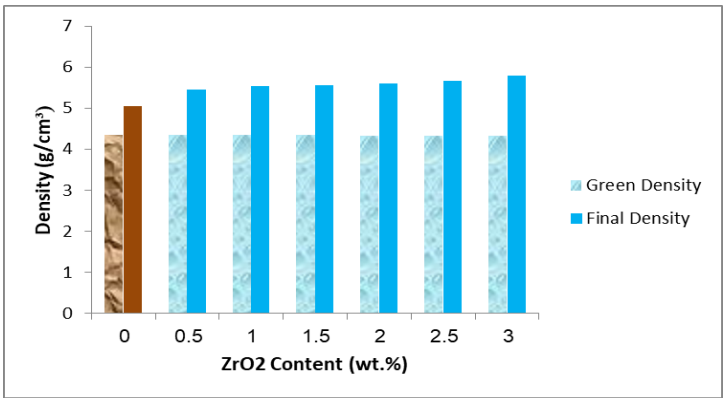

Fig. 5. Effect of ZrO_2 Final Porosity

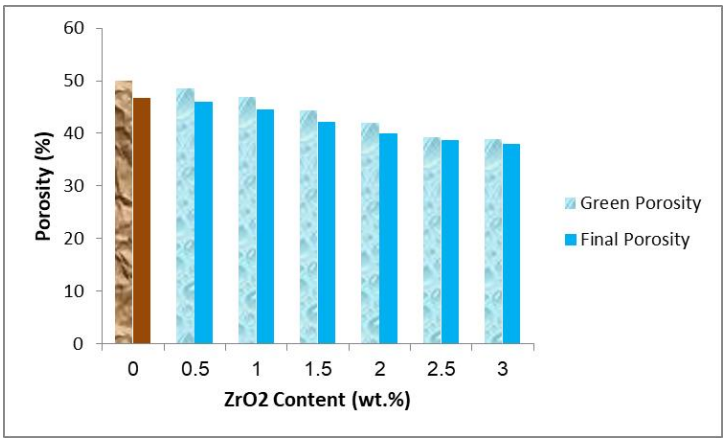

Fig. 6. Effect of ZrO_2 on Final Porosity

10.4. SCANNING ELECTRONE MICROSCOPE

Due to the high sensitivity of SEM images to chemical composition, the sintered specimen's microstructure reveals two phases (α-Zr and β-Zr) of a multiphase structure. SEM is done in order to investigate the chemical composition of the desired point. Fig.7-a, shows the SEM images for the base alloy. Fig.7-b, illustrates the SEM image of $Zr2.5Nb3ZrO_2$ specimen, its showed the effect of adding Zirconia on microstructure, the white particles refer to zirconia and are scattered regularly in the matrix. The multiphase appearance of α and β phases means the success of the manufacturing process by powder metallurgy. The results of the SEM showed results agree with X-ray diffraction.

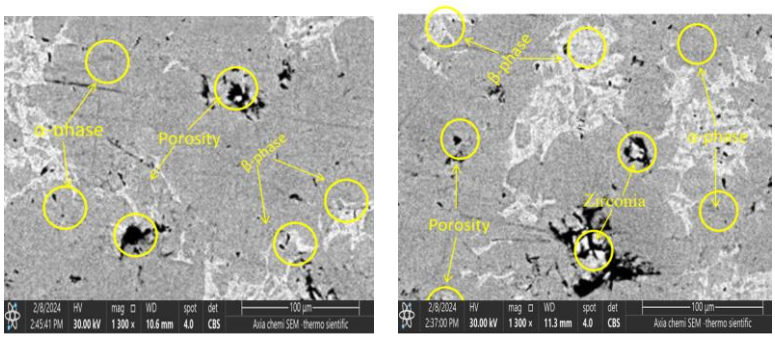

(a) **(b)**

Fig. 7. SEM Images for (a) Base Alloy and (b) B6 Alloy

10.5. HARDNESS TEST

Brinell hardness was measured for all alloys. Fig.8, illustrates the influence of zirconia addition on hardness, it can be seen that hardness raises with raising zirconia content ,this is due to the fact to the addition of zirconia particles that strengthening the solid solution by impending the dislocation movement.

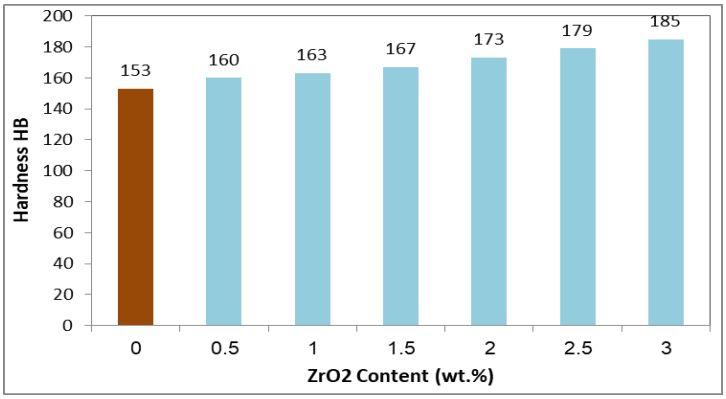

Fig. 8. Effect of ZrO_2 on Hardness

10.6. DRY WEAR TEST

This test has been carried out on samples with a diameter of (13) mm using different loads (10, 15, 20) N and with the different durations of time (5,10,15,20,25,30, 35,40 and 45) min. Figs.9-14 showed the volume loss VS time and wear rate VS time for all samples under different loads. An increase in load that has been applied to the sample increased rate of wear. The wear rate is the highest value at which the applied load is 20 N. This is due to the fact that the weight loss rises when a high load is applied because of the friction on the surface increase and the removal of the material is more when the applied load increases, because contact pressure and temperature between sample and the steel pin increase.

When adding ceramic particles to the alloy, it will improve the wear resistance because of its high hardness that resists friction and this is clear in the Fig.9 to 14 where the influence of adding zirconia on the rate of wear was observed. Increasing the amount of zirconia to 3% had resulted in a decrease in wear rate.

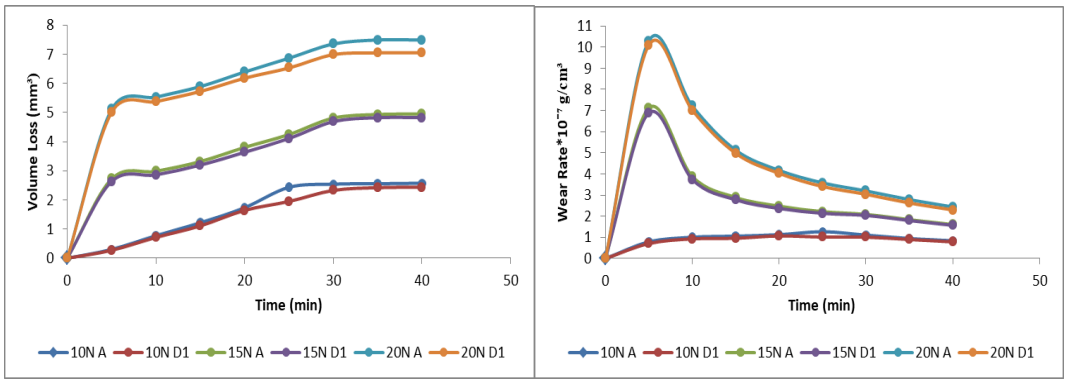

Fig. 9. Volume Loss and Wear Rate with Time Under Different Applied Loads for Base and B1 Alloys

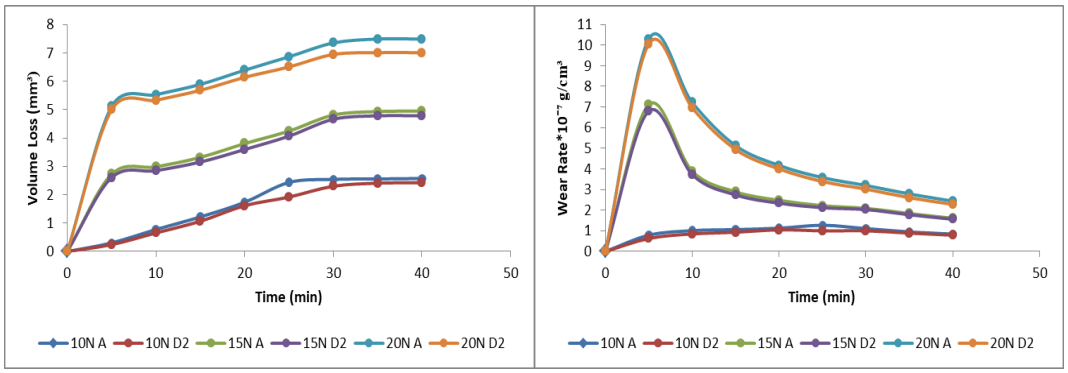

Fig. 10. Volume Loss and Wear Rate with Time Under Different Applied Loads for Base and B2 Alloys

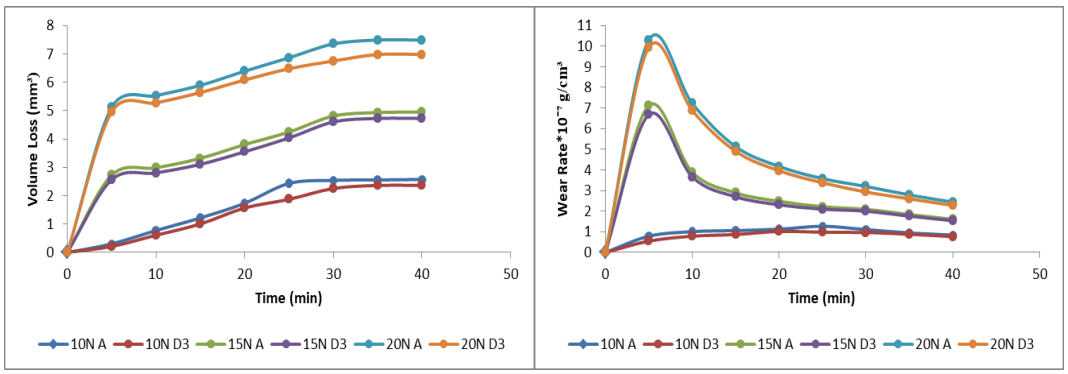

Fig. 11. Volume Loss and Wear Rate with Time Under Different Applied Loads for Base and B3 Alloys

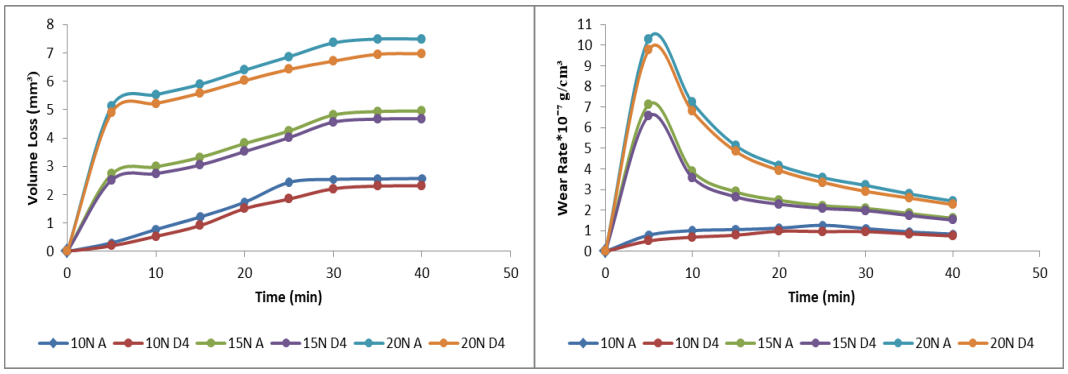

Fig. 12. Volume Loss and Wear Rate with Time Under Different Applied Loads for Base and B4 Alloys

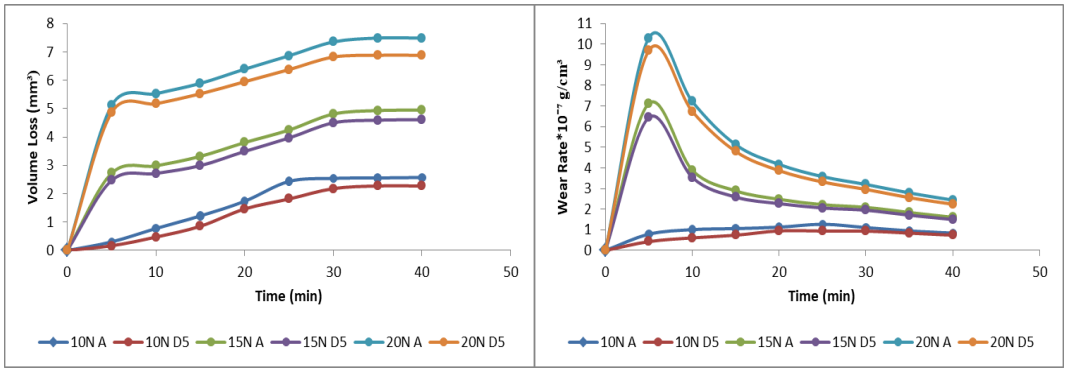

Fig. 13. Volume Loss and Wear Rate with Time Under Different Applied Loads for Base and B5 Alloys

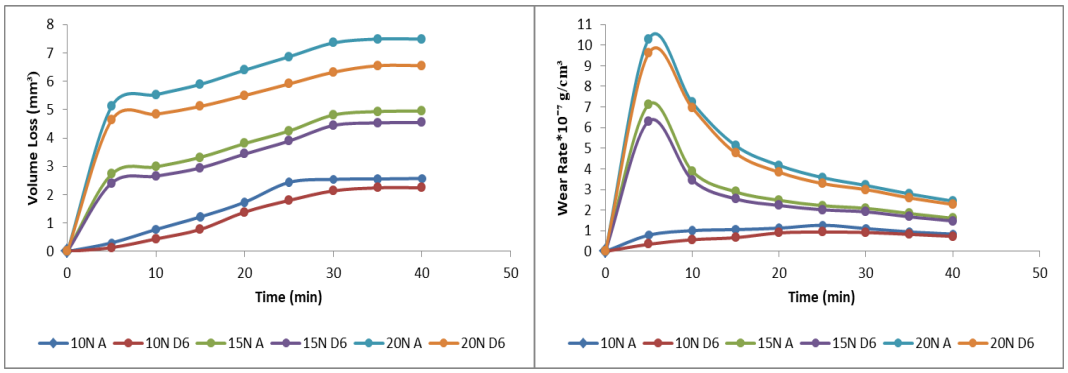

Fig. 14. Volume Loss and Wear Rate with Time under Different Applied Loads for Base and B6 Alloys

11. CONCLUSION

1- The best compacting pressure for Zr2.5Nb alloy that used in this work was 800 MPa, in this compacting pressure obtained the least porosity and the highest density of the compacted sample.

2- The sintering process for 8hr. at 1100° C of specimens (with and without additives) is enough to finish the transformation process of Zr and Nb to alloy structure.

3- Only two phases were appeared at room temperature in all alloys (with and without additives), α-Zr and β-Zr.

4- The addition of ZrO_2 with (0.5, 1, 1.5, 2, 2.5 and 3) wt. % to Zr2.5Nb alloy resulted in decreasing the wear rate.

12. REFEREANCES

Antunes, R.A. and de Oliveira, M.C.L. (2012) 'Corrosion fatigue of biomedical metallic alloys: mechanisms and mitigation', Acta Biomaterialia, 8(3), pp. 937–962.

ASTM B328 (2003) 'Standard Test Method for Density. Relative Density (Specific Gravity), and Absorption of Fine Aggregate.'

Di Girolamo, G., Brentari, A., Blasi, C. and Serra, E. (2014) 'Microstructure and mechanical properties of plasma sprayed alumina-based coatings', Ceramics International, 40(8), pp. 12861–12867.

Gittens, R.A., Olivares-Navarrete, R., Schwartz, Z. and Boyan, B.D. (2014) 'Implant osseointegration and the role of microroughness and nanostructures: lessons for spine implants', Acta Biomaterialia, 10(8), pp. 3363–3371.

Hou, G., An, Y., Zhao, X., Zhou, H., Chen, J., Li, S. and Deng, W. (2017) 'Improving interfacial, mechanical and tribological properties of alumina coatings on Al alloy by plasma arc heat-treatment of substrate', Applied Surface Science, 411, pp. 53–66.

Hyson Jr, J.M. (2006) 'Amalgam: Its history and perils', Journal of the California Dental Association, 34(3), pp. 215–229.

Kumar, S., Kumar, A., Kumar, D. and Jain, J. (2017) 'Thermally sprayed alumina and ceria-doped-alumina coatings on AZ91 Mg alloy', Surface and Coatings Technology.

Kunčická, L., Kocich, R. and Lowe, T.C. (2017) 'Advances in metals and alloys for joint replacement', Progress in Materials Science, 88, pp. 232–280.

Manivasagam, G., Dhinasekaran, D. and Rajamanickam, A. (2010) 'Biomedical implants: corrosion and its prevention—a review', Recent Patents on Corrosion Science, 2, pp. 40–54.

Mo, M.-H., Wu, L.-K., Cao, H.-Z., Lin, J.-P., Zheng, G.-Q. (2017) 'Halogen effect for improving high temperature oxidation resistance of Ti-50Al by anodization', Applied Surface Science, 407, pp. 246–254.

Narayanan, T.S. and Seshadri, S.K. (2000) 'Cathodic electrosynthesis of alumina thin films and powders', Journal of Materials Science Letters, 19(19), pp. 1715–1718

Niinomi, M., Narushima, T. and Nakai, M. (eds.) (2015) Advances in Metallic Biomaterials: Tissues, Materials and Biological Reactions. Vol. 3. Springer.

Sara, M.G. (2015) Effect of (Cu & Cr) Additives on Corrosion and Dry Sliding Wear of NiTi Shape Memory Alloy. MSc thesis. College of Materials Engineering, University of Babylon, Iraq.

Tianshuo, S., Shuguang, L., Bohan, C., Ziyao, C., Xianrui, Z., Shiliang, Z., Qiang, L. and Chaoqun, X. (2024) 'Wear and corrosion resistance behavior of Zr-2.5Nb by pack carburizing and boronizing', Surface and Coatings Technology, 482.